MRS Communications (2017), 7, 677–682
© Materials Research Society, 2017
doi:10.1557/mrc.2017.70

MRS Communications

Research Letter

Densification of thoria through flash sintering

W. Straka, Department of Materials Science and Engineering, North Carolina State University, Raleigh, NC 27606, USA
S. Amoah, Department of Materials Science and Engineering, North Carolina State University, Raleigh, NC 27606, USA; Department of Physics, Lenoir Rhyne University, Hickory, NC 28601, USA
J. Schwartz, Department of Materials Science and Engineering, North Carolina State University, Raleigh, NC 27606, USA

Address all correspondence to W. Straka at **wjstraka@ncsu.edu**

(Received 8 May 2017; accepted 2 August 2017)

Abstract

Thorium dioxide (thoria, ThO_2) is used in refractory applications and as nuclear fuel. Its melting temperature, the highest of any binary oxide, makes it a difficult system to process. Here we report on the effects of flash sintering on the densification of thoria. We found 95% of theoretical density is obtained at ~950 °C (~30% of the melting temperature) with an electric field of 800 V/cm. Variation in power density had a minimal effect on the densification. Scanning electron microscopy images show the effects of flash sintering on grain size as a function of electric field.

Introduction

Thorium dioxide (thoria, ThO_2) is a binary oxide ceramic with the highest melting temperature of any known binary oxide.[1,2] As a result, thoria is an important refractory material for many applications. Furthermore, thoria is an important nuclear fuel in several countries because it is more abundant than uranium, is nuclear proliferation-resistant, and can produce more energy per unit mass than uranium-based fuels.[3] Although its high melting temperature is one of thoria's attractive features, it also makes it difficult to obtain the fully-dense materials required for refractory and nuclear applications, and in general processing thoria is challenging.

To overcome the processing barrier, many techniques have been investigated to find their efficacy for thoria sintering. Examples of this include variation in the sintering atmosphere[4,5] and reduction in particle size.[6,7] At best, these studies yielded dense thoria at temperatures exceeding 1600 °C.[5] Another thoria densification method involves the addition of sintering aids such as alumina,[5] niobia,[8,9] calcia,[6] vanadia, and tantala.[10] Of these, niobia, vanadia, and tantala yielded the most promising results with theoretical densities exceeding 95% with sintering temperatures between 1150 and 1200 °C.[8–10] Because the nuclear industry requires pure thoria for use as a nuclear fuel; however, the addition of a sintering aid must be avoided for nuclear applications. Additionally, the addition of cations with different oxidation states from thorium results in the creation of oxygen interstitials and vacancies. To avoid contamination, two studies have considered the effect of an electric field on the densification of thoria.[11,12] In particular, these investigations studied spark plasma sintering on thoria and thoria–urania complexes and reported their final densities. Both of these studies achieved 96% theoretical dense pellets at temperatures of 1600 °C. More recently, a new study looking into mechanisms of flash sintering studied the onset for uranium dioxide (UO_2) pellets.[13] To date, no study has reported dense thoria pellets at sintering temperatures below 1600 °C without the use of sintering aids.

One technique with the potential to reduce the sintering temperature of thoria is flash sintering. First discovered by Cologna et al.,[14] flash sintering involves heating a ceramic sample, while it is subjected to a constant DC electric field. As the temperature increases, the sample resistivity decreases slowly at first and then abruptly, resulting in a "flash" from the power supply when the current increases quickly (typically to the maximum current the power supply can output) and the electric field (or voltage) begins to decrease. In a few seconds, the density of the ceramic reaches near theoretical density. The combination of electric field and temperature at which the ceramic quickly densifies is material dependent. This technique is different from the field-assisted sintering technique (FAST) in that the electric field for flash sintering is higher and the onset of sintering occurs at a lower temperature than in conventional sintering. The origins of this mechanism have been studied via flash sintering and non-flash sintering experiments with several theories being proposed including, but not limited to: Joule heating,[14] the creation of Frenkel pairs,[15,16] migration of the pores,[17] defect redistribution,[18,19] and thermal runaway.[20–23] In a typical experiment, a dog-bone-shaped sample with holes in the ends is suspended by wires that transmit the electric field.[24] Using this technique, cubic zirconia has been sintered at 390 °C (conventional sintering temperature of 1400 °C),[25] Co_2MnO_4 at 325 °C (conventional sintering temperature of 1100 °C),[26] and alumina doped with magnesia at 1260 °C (conventional sintering temperature of 1700 °C).[16]

https://doi.org/10.1557/mrc.2017.70 Published online by Cambridge University Press

Here we investigate the effects of the primary flash sintering variables, electric field, and current on the densification of thoria. Through these studies, the flash temperatures are identified, as are the effects on grain size and final density.

Experimental approach

Thoria powder was synthesized by mixing 0.25 mol of thorium nitrate hydrate (Sigma-Aldrich 99% ~5 mol/mol water) and 0.5 mol of oxalic acid (Sigma-Aldrich >99% ReagentPlus) into 1 L of deionized water. The solution was stirred and allowed to react for 12 h in air. The resulting thorium oxalate precipitate was vacuum filtered through Whatman No. 42 ashless paper, and then washed with additional deionized water. The thorium oxalate was then dried at 120 °C for 12 h and calcined at 600 °C for 24 h in air with a ramp rate of 20 °C/min. The resulting thoria powder was ball milled for 8 h in a planetary ball mill at 3 Hz using a 30:1 weight ratio of zirconia milling media to powder in a polyethylene jar. After milling, the powder was separated from the milling media using a 140 μm sieve. Cylindrical pellets (6 mm diameter, 3.75 mm height) were formed in a Carver uniaxial press at 1 GPa. Densities of the green pellets were measured geometrically, whereas the densities of the sintered pellets were measured using the Archimedes method. On some pellets, silver paint (SPI high-purity silver paint) was painted onto the ends of the pellet and baked at 60 °C in air to ensure even electric field distribution.

Flash sintering was performed in a dilatometer fitted to apply an electric field and provide electric current to the ceramic pellets. First, the system was calibrated to minimize the effects of noise. A thoria pellet was placed between two platinum electrodes that were attached to one of two power supplies (Glassman High Voltage power supply, model PS/PG-003R-250 and Sorensen DCS300-3.5). A linear variable differential transducer (LVDT) was used to measure the real-time change in length of the pellet. A type-N thermocouple was placed within 2 mm of the sample to measure the temperature near the sample. Keithley 2700 DMMs were used to measure the current and voltage passed to the pellet, the displacement from the LVDT, and the temperature near the pellet. The DMMs were attached to a computer via GPIB and data were collected using LabView. For all experiments, the electric field was held constant, while the temperature ramped. Once the current limit was reached, the power supply and furnace were allowed to run for an additional 10 s before being switched off.

To study the effect of the magnitude of the electric field on densification, green thoria pellets were heated with 533.3, 800.0, 1066.7, 1333.3, and 1600.0 V/cm electric fields. The maximum current limits were set as 338, 225, 169, 135, and 113 mA, respectively, to maintain a max power density for all pellets of 635 mW/mm^3. An additional pellet was annealed with no electric field applied at the same ramp rate to 1250 °C and held for 10 s as a comparison with the pellets subjected to the electric field. Some pellets had silver paint dried onto the ends to ensure a uniform electric field.

Powder x-ray diffraction (XRD, Rigaku Geigerflex) and dynamic light scattering (DLS, Malvern Zetasizer Nano ZSP) were used to confirm phase purity and to measure the starting particle size of the sample, respectively. Pellets were polished to a 0.1 μm finish with diamond paste. Scanning electron microscope (SEM) images were taken of the polished pellets using a Hitachi S4800 electron microscope with energy-dispersive x-ray spectroscopy (EDS). Grain size analysis was done via the line intercept method.

Results and discussion

Powder XRD was done on the synthesized thoria powder and it matched the standard given by Wyckoff [27] indicating phase pure thoria. To ensure no zirconia impurities from the milling media, EDS was also done and, to the detection limits of the EDS detector, no zirconia was seen. DLS was used to measure the particle sizes of the starting powder and, using a Gaussian distribution, showed an average size of 265.04 nm with an error of 68.90 nm. These starting particle sizes were the largest that would be present in the starting powder and may be larger than an actual average particle size due to DLS's inability to distinguish between agglomerations and single particles. The XRD spectrum, EDS spectrum, and DLS particle size distributions are all in the appendix as Figs. S1–S3, respectively. All pellets had a green density of 67% with a SD of 0.5%.

Figure 1 illustrates the sintering curves for pellets coated with silver as a function of temperature; both the normalized change in length and the power to the pellet are shown. For this figure and all subsequent discussion and figures, the temperature indicated is measured from a thermocouple located 2 mm away from the sample. It gives an approximation of the temperature of the ceramic rather than the furnace temperature. However, because the thermocouple is not actually touching the ceramic, its true temperature is difficult to know.

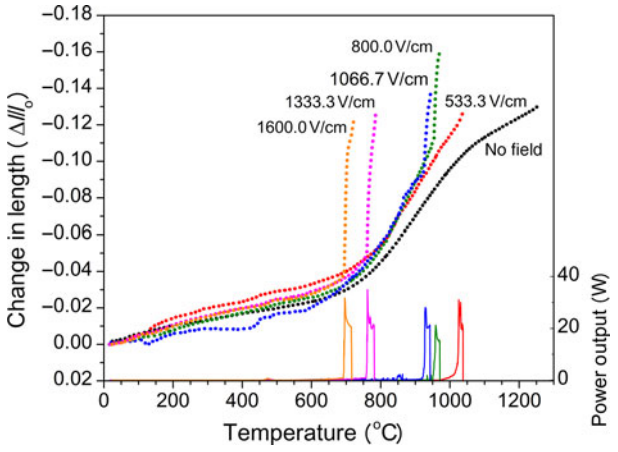


Figure 1. Flash sintering curves for thoria pellets, showing the normalized change in length as a function of temperature for various applied electric fields. The power output from the power supply corroborates the sudden change in length seen during the sintering process.

https://doi.org/10.1557/mrc.2017.70 Published online by Cambridge University Press

The electric field magnitude for these sintering curves in Fig. 1 varies from 0 to 1600 V/cm. As seen in Fig. 1, the sintering curve for a pellet subjected to 533.3 V/cm follows closely the normal sintering curve for this ceramic. Figure 2 shows an Arrhenius plot of the normalized power through the pellet at a given temperature. This plot is meant to illustrate whether the ceramic is undergoing a "flash" event or whether the current is rising due to decreased resistivity at elevated temperatures. For the ceramics subjected to field magnitudes at and >800 V/cm, there appears a discontinuity in the power applied as temperature rises (a sudden jump upward in normalized power applied). This discontinuity is indicative of a "flash" event. For the ceramic subjected to a field of 533.3 V/cm, there was no immediate discontinuity but a slow increase in the power applied to the pellet. This indicates FAST sintering instead of flash.[26] Non-zero electric fields below 533.3 V/cm only showed the FAST sintering regime and are not included in the data presented.

One of the prevailing theories behind flash sintering is that thermal runaway induces the full densification of the ceramic. Based on the analysis by Dong and Chen[23] the onset furnace temperature and electric field for each condition were used and plotted based on their method. From this plot, as shown in Fig. 3(a), the activation energy of the conductivity of thoria (the slope of the plot) was calculated to be 1.002 eV, which compares with values seen in literature of between 0.85 and 1.5 eV.[28–31] The *y*-value of this plot at 1000 K was also calculated to be −12.99 $V^2/cm^2/K^4$, which places this material in the middle of the oxygen ion conductors in.[23] The other isostructural oxides are well-known ion conductors whose conduction mechanism is controlled by oxygen vacancies leading to cation diffusion.[32,33] Oxygen vacancies can be created through dopants[34,35] or through the creation of anion Frenkel pairs. As the current system was undoped, was processed in air, and thorium is absent of oxidation states other than 4^+, cation diffusion was enhanced by an increase in the number of oxygen vacancies,[33] which has been shown to be enhanced with the application of an electric field.[36] An additional method for the increase in cation diffusion could be through the creation of cation vacancies. This has been shown in a recent study by Raftery[13] where the onset conditions for flash sintering of UO_2 were studied as a function of the stoichiometry of urania. In particular, the oxygen content was varied in these pellets to go from pure UO_2 to hyperstoichiometric mixes. Although UO_2 and thoria are isostructural with the same oxidation state, uranium can have an additional 5^+ oxidation state, which can accommodate additional oxygen in the lattice. As thorium is absent of other oxidation states, it seems unlikely that the stoichiometry varied in the current system. This makes the most likely explanation that

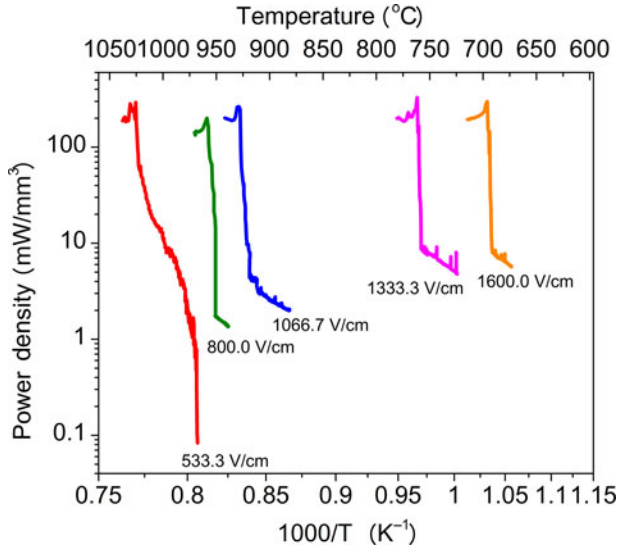


Figure 2. Arrhenius plots of the power density for various electric fields during flash sintering. The sample annealed with 533.3 V/cm field shows some FAST characteristics as is evidenced by the curvature in the power density as a function of temperature.

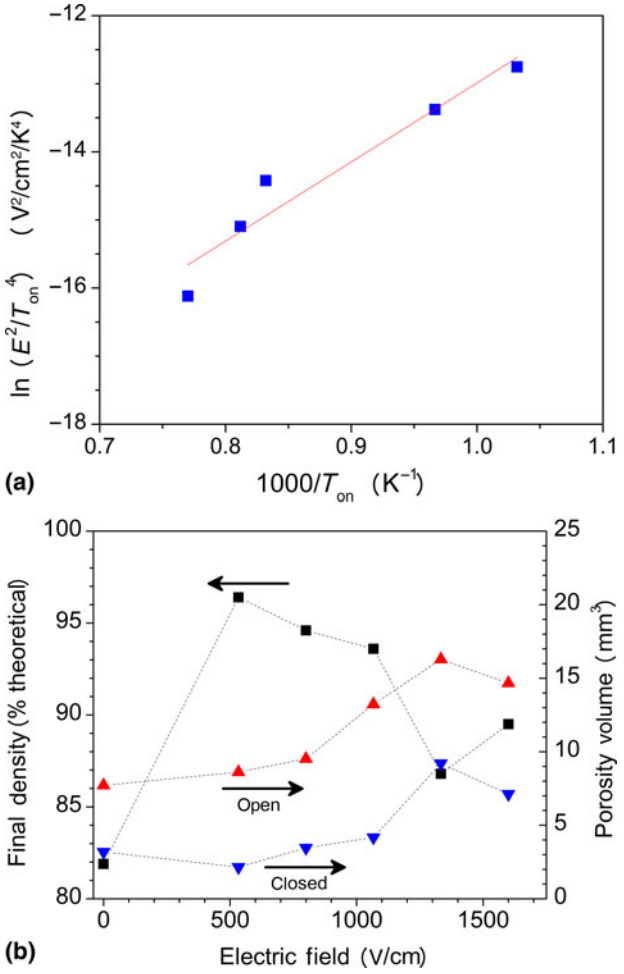


Figure 3. (a) Plot of the flash sintering data plotted as per[23] with the slope giving the activation energy, and (b) the final density and porosity volumes for the pellets as a function of electric field. The dashed lines in (b) are shown only as guides for the eye.

https://doi.org/10.1557/mrc.2017.70 Published online by Cambridge University Press

the electric field enhanced the creation of oxygen vacancies and interstitials, which lead to higher cation diffusion as the mechanism for densification of thoria. Figure 3(b) shows the final density, open porosity volume, and closed porosity volume for each thoria pellet processed at the shown electric fields.

Figure 4 shows SEM micrographs of the polished pellet cross-sections for pellets processed in electric fields ranging from zero to 1600 V/cm. Visual inspection shows minimal changes in microstructure due to the electric field. Subsequent grain size analysis shows that at higher electric fields, smaller grain sizes are retained, which is to be expected because higher electric field is also associated with lower sintering temperature. The particle size distributions for each pellet sintered at the given electric fields were fitted with a Gaussian distribution. These distributions are shown in the appendix as Fig. S4. From each distribution, an average grain size was calculated for each condition along with its SE. The average grain sizes measured for pellets with applied electric field magnitudes of 0, 533.3, 800, 1066.7, 1333.3, and 1600 V/cm were 262.99 ± 95.37, 224.93 ± 30.68, 180.55 ± 53.90, 174.03 ± 57.61, 57.37 ± 14.79, and 55.03 ± 13.98 nm, respectively. The final grain sizes in these cross-sectional images elude to agglomerations in the starting powder. The particle sizes shown in these plots elude to agglomerations in the starting powder. The mean particle size seen in the SEM images for each thoria pellet processed at different electric fields was compared with the measured maximum temperature of the pellet (Fig. 5). Because the thoria processed at higher electric fields densified at lower temperatures, the maximum temperature experienced by that pellet is lower. The SD for each mean

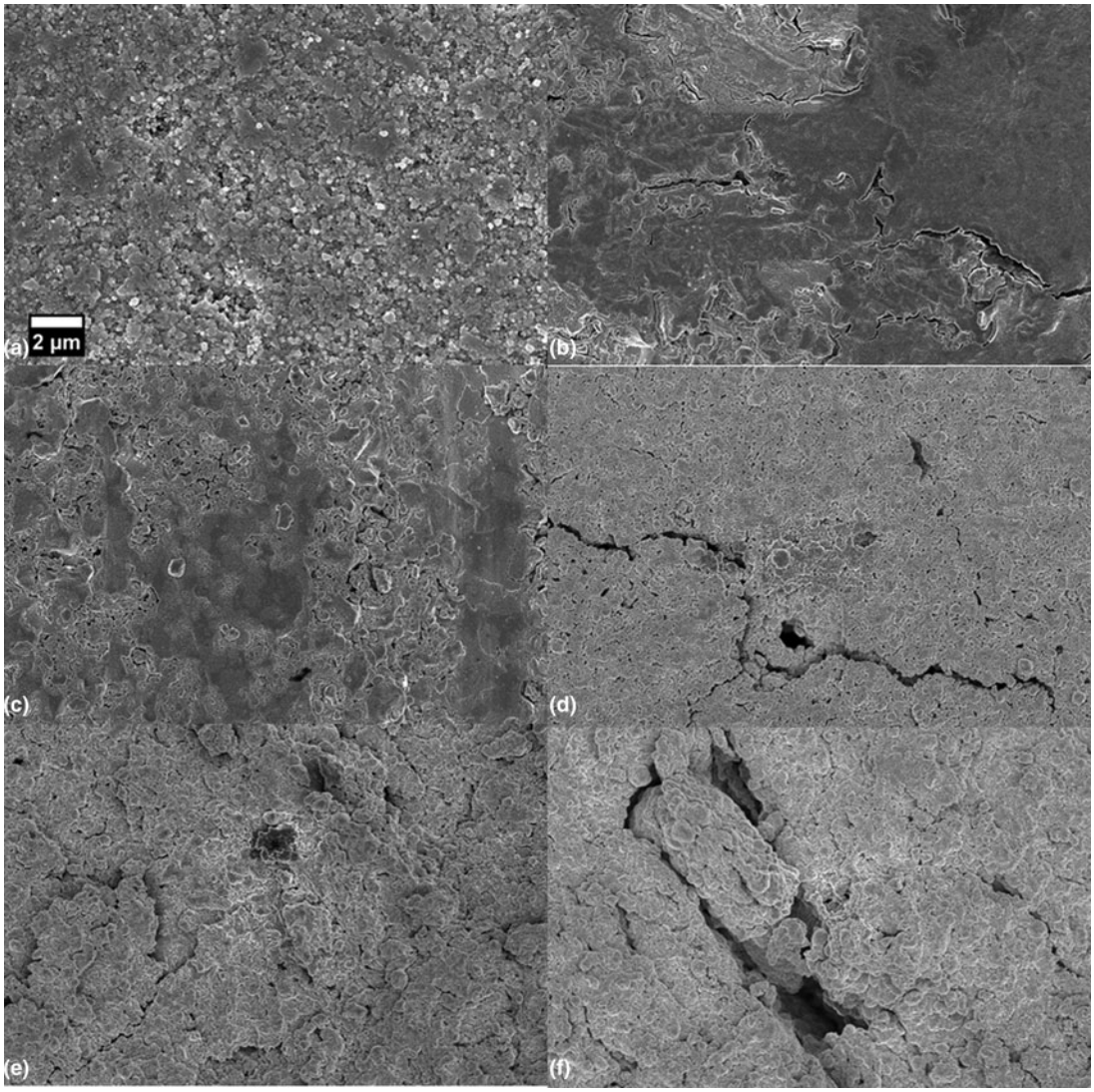


Figure 4. SEM micrographs of polished thoria samples for: (a) 0 V/cm, (b) 533.3 V/cm, (c) 800 V/cm, (d) 1066.7 V/cm, (e) 1333.3 V/cm, and (f) 1600 V/cm. Note that the scale bar applies to all images.

https://doi.org/10.1557/mrc.2017.70 Published online by Cambridge University Press

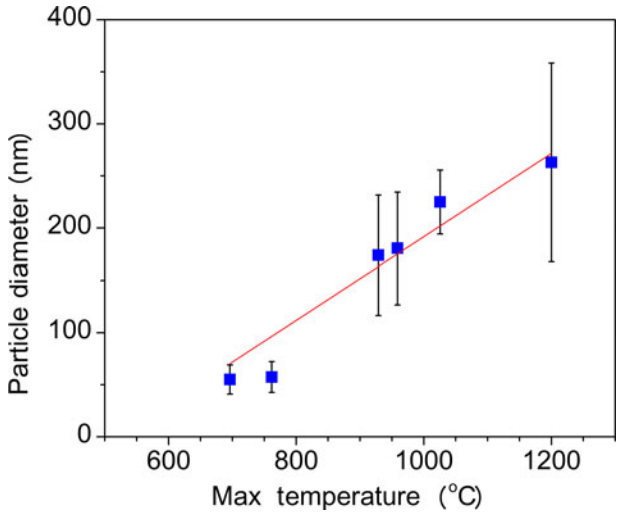


Figure 5. Particle size as a function of maximum observed temperature of each pellet. The error bars are for average particle size. A line was fitted to this curve using least-squares method.

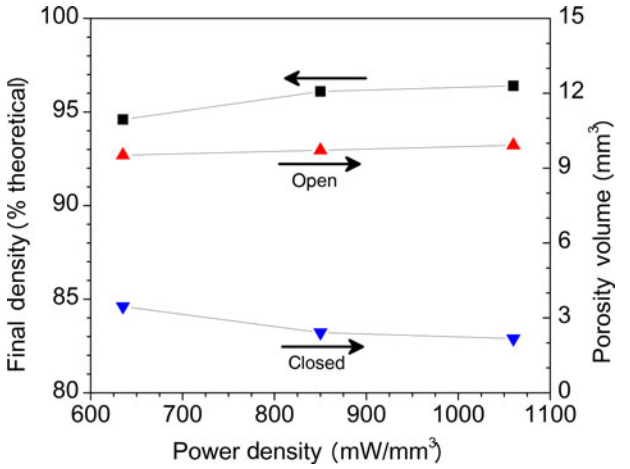


Figure 6. Final pellet density and porosity volumes as a function of electric field. The dashed lines are shown only as guides for the eye.

particle size is plotted as error bars and the points were fit linearly to find a correlation. The r^2 value was calculated to be 0.932.

To this point, all thoria pellets were coated with silver paint in order to maintain an evenly applied electric field across the sample surface. For thoria's use as a nuclear fuel, thoria processing must minimize elemental contamination. As a result, thoria pellets were flash sintered with and without silver paint on the ends of the pellets. The flash temperatures of the pellets without silver paint were significantly higher than pellets with silver paint. The sintering curves for these pellets are shown in the appendix as Fig. S5. Furthermore, the pellets without silver paint appear to have localized electrical breakdown indicated by a hole melted through the thoria pellet. The most likely reason for the observed melting is the enormous current density through the pellet. In the prior experiments (thoria pellets with silver paint on their surface), the current was applied evenly across the sample cross-section. With no silver paint, the current passed through an extremely small spot; most likely, the diameter of the hole melted through the material. This would result in a power density through that localized area of more than 50,000 mW/mm^3. This result necessitates the use of some conductive medium on the surface of the ceramic. The sintering curves with the power output as a function of temperature for pellets coated with silver and not coated with silver are shown in the online appendix.

Although results for electric fields greater than 800 V/cm are shown, it is important to note that when processing at electric fields above this field, pellets would typically break apart. This occurred regardless of the power density applied to the pellet. As a result, to study the effects of power density on the densification, the electric field was held constant at 800 V/cm and the power was varied by varying the current; power densities studied were 635, 850, and 1060 mW/mm^3. The resulting final densities, open porosity volumes, and closed porosity volumes are shown in Fig. 6. Interestingly, power density has a relatively weak effect on densification and open porosity volume. It does, however, have a more significant effect on the closed porosity volume. An increase in the power density decreased the closed porosity volume. This trend is opposite that seen with an increase in the electric field.

These results illustrate that flash sintering is an effective approach for densifying thoria, as densities of 95% theoretical density are obtained at temperatures below 1000 °C. The results show that the final density of the thoria pellets was higher for the ceramics processed at lower electric fields, most likely due to the higher flash temperature; thus there is a materials-dependent optimum balance between temperature and electric field. Furthermore, these results show that for low values of electric field, samples undergo FAST sintering, but as the electric field increases there is a transition to flash sintering. From the Arrhenius plot, for the case of thoria, the transition occurs at an electric field of about 533.3 V/cm. All of the above results assume a perfect stoichiometric mix of thorium and oxygen. As has been observed in prior studies, an excess of oxygen in the ceramic could lead to even lower temperatures for sintering followed by a reoxygenation.

A prior study investigated the effects of the electrode composition on the sintering temperature, final density, and porosity of alumina. This study found that the onset of flash sintering was lower for silver paint than for carbon cement or for platinum paste.[37] Here we considered the effects of the presence of conductive silver paint applied directly to the thoria pellet. In the absence of silver paint, electrical breakdown was evident due to uneven contact between the platinum electrode and the ceramic body, resulting in localized electrical contact, non-uniform and limited current distribution, and a locally high-power density on the face of the pellet. In comparison, the addition of conductive silver paint mitigates the non-uniform electrical contact and

https://doi.org/10.1557/mrc.2017.70 Published online by Cambridge University Press

results in a uniform distribution of the electric field, preventing localized breakdown and more uniform densification.

Conclusions

Flash sintering is an effective sintering technique for the densification of thoria, which has the highest sintering temperature of all binary oxides. The careful selection of the electric fields is essential for flash sintering. In the case of thoria, for electric fields below about 533.3 V/cm, flash sintering does not occur and instead the sample remains in the FAST sintering regime. In addition, if the electric field is above 800 V/cm, the thoria pellets tended to break. This study also shows the benefits of coating the surface of the ceramic with conductive media to obtain a more-uniform flash sinter. Additionally, while the current seems to have an effect on the final density of the thoria pellets, this effect is relatively small.

Supplementary material

The supplementary material for this article can be found at https://doi.org/10.1557/mrc.2017.70.

Acknowledgments

The authors thank Roger Russell and Toby Tung for their help with the experimental setup, the Clemson University Electron Microscopy Laboratory for allowing us to utilize their SEMs, and Brian Powell for his assistance in acquiring the electron images. In addition, we acknowledge NSF support for the REU on Advanced Materials for Environmental Sustainability under grant EEC 1156762 which funded one of the authors (S. A.).

References

1. C. Ronchi and J.P. Hiernaut: Experimental measurement of pre-melting and melting of thorium dioxide. *J. Alloys Compd.* **240**, 179–185 (1996).
2. S. Peterson, R.E. Adams, and D.A. Douglas: Properties of thorium, its alloys, and its compounds. In *Utilization of Thorium in Power Reactors*, International Atomic Energy Agency (IAEA) Technical reports series No. 52 (IAEA, Vienna, Austria, 1966), pp. 292–312.
3. L.B. Amgaonkar, M.V. Rathod, A.P. Pardey, and S.P. Khandait: Thorium as a nuclear fuel. *Int. J. Eng. Appl. Technol.* AGNIPANKH-15, 48 (2015).
4. J.M. Pope and K.C. Radford: Physical properties of some thoria powders and their influence on sinterability. *J. Nucl. Mater.* **52**, 241–254 (1974).
5. A. Baena, T. Cardinaels, J. Vleugels, K. Binnemans, and M. Verwerft: Activated sintering of ThO_2 with Al_2O_3 under reducing and oxidizing conditions. *J. Nucl. Mater.* **470**, 34–43 (2016).
6. K. Ananthasivan, S. Balakrishnan, S. Anthonysamy, R. Divakar, E. Mohandas, and V. Ganesan: Synthesis and sintering of nanocrystalline thoria doped with CaO and MgO derived through oxalate-deagglomeration. *J. Nucl. Mater.* **434**, 223–229 (2013).
7. V. Chandramouli, S. Anthonysamy, P.R. Vasudeva Rao, R. Divakar, and D. Sundararaman: PVA aided microwave synthesis: a novel route for the production of nanocrystalline thoria powder. *J. Nucl. Mater.* **231**, 213–220 (1996).
8. P. Balakrishna, B.P. Varma, T.S. Krishnan, T.R.R. Mohan, and P. Ramakrishnan: Thorium-oxide—calcination, compaction and sintering. *J. Nucl. Mater.* **160**, 88–94 (1988).
9. P. Balakrishna, B.P. Varma, T.S. Krishnan, T.R.R. Mohan, and P. Ramakrishnan: Low-temperature sintering of thoria. *J. Mater. Sci. Lett.* **7**, 657–660 (1988).
10. K. Ananthasivan, S. Anthonysamy, C. Sudha, A.L.E. Terrance, and P.R. V. Rao: Thoria doped with cations of group VB-synthesis and sintering. *J. Nucl. Mater.* **300**, 217–229 (2002).
11. H. Muta, Y. Murakami, M. Uno, K. Kurosaki, and S. Yamanaka: Thermophysical properties of Th1-xUxO_2 pellets prepared by spark plasma sintering technique. *J. Nucl. Sci. Technol.* **50**, 181–187 (2013).
12. V. Tyrpekl, M. Cologna, D. Robba, and J. Somers: Sintering behaviour of nanocrystalline ThO_2 powder using spark plasma sintering. *J. Eur. Ceram. Soc.* **36**, 767–772 (2016).
13. A.M. Raftery, J.G. Pereira da Silva, D.D. Byler, D.A. Andersson, B. P. Uberuaga, C.R. Stanek, and K.J. McClellan: Onset conditions for flash sintering of UO_2. *J. Nucl. Mater.* **493**, 264–270 (2017).
14. M. Cologna, B. Rashkova, and R. Raj: Flash sintering of nanograin zirconia in < 5 s at 850 °C. *J. Am. Ceram. Soc.* **93**, 3556–3559 (2010).
15. J.S.C. Francis, M. Cologna, and R. Raj: Particle size effects in flash sintering. *J. Eur. Ceram. Soc.* **32**, 3129–3136 (2012).
16. M. Cologna, J.S.C. Francis, and R. Raj: Field assisted and flash sintering of alumina and its relationship to conductivity and MgO-doping. *J. Eur. Ceram. Soc.* **31**, 2827–2837 (2011).
17. S. Kim, S.L. Kang, and I. Chen: Electro-sintering of yttria-stabilized cubic zirconia. *J. Am. Ceram. Soc.* **96**, 1398–1406 (2013).
18. W. Rheinheimer, M. Fülling, and M.J. Hoffmann: Grain growth in weak electric fields in strontium titanate: grain growth acceleration by defect redistribution. *J. Eur. Ceram. Soc.* **36**, 2773–2780 (2016).
19. W. Qin, H. Majidi, J. Yun, and K. van Benthem: Electrode effects on microstructure formation during FLASH sintering of yttrium-stabilized zirconia. *J. Am. Ceram. Soc.* **99**, 2253–2259 (2016).
20. J.G. Pereira da Silva, H.A. Al-Qureshi, F. Keil, and R. Janssen: A dynamic bifurcation criterion for thermal runaway during the flash sintering of ceramics. *J. Eur. Ceram. Soc.* **36**, 1261–1267 (2016).
21. R.I. Todd, E. Zapata-Solvas, R.S. Bonilla, T. Sneddon, and P.R. Wilshaw: Electrical characteristics of flash sintering: thermal runaway of Joule heating. *J. Eur. Ceram. Soc.* **35**, 1865–1877 (2015).
22. Y. Dong and I. Chen: Predicting the onset of flash sintering. *J. Am. Ceram. Soc.* **98**, 2333–2335 (2015).
23. Y. Dong and I.W. Chen: Onset criterion for flash sintering. *J. Am. Ceram. Soc.* **98**, 3624–3627 (2015).
24. S.K. Jha, J.M. Lebrun, and R. Raj: Phase transformation in the alumina–titania system during flash sintering experiments. *J. Eur. Ceram. Soc.* **36**, 733–739 (2016).
25. J.A. Downs and V.M. Sglavo: Electric field assisted sintering of cubic zirconia at 390 degrees C. *J. Am. Ceram. Soc.* **96**, 1342–1344 (2013).
26. A.L.G. Prette, M. Cologna, V. Sglavo, and R. Raj: Flash-sintering of Co_2MnO_4 spinel for solid oxide fuel cell applications. *J. Power Sources* **196**, 2061–2065 (2011).
27. R.W.G. Wyckoff: *Crystal Structures* (John Wiley, New York, 1963).
28. H.S. Maiti and E.C. Subbarao: Electrical-conduction in CaO-doped thoria electrolytes. *J. Electrochem. Soc.* **123**, 1713–1718 (1976).
29. W.E. Danforth and F.H. Morgan: Electrical resistance of thoria. *Phys. Rev.* **79**, 142–144 (1950).
30. M. Iqbal and E.H. Baker: Conductivity measurements on thoria and thoria—yttria solid solutions at high oxygen pressures. *High Temp. Press.* **5**, 265–271 (1973).
31. A. Hammou and C. Deportes: Electrical conductivity and defects structure in thorium-dioxide at high-temperature: study of ionic and electronic conductivities. *J. Chime Phys. Phys.-Chim. Biol.* **71**, 1071–1080 (1974).
32. M. Aizenshtein, T.Y. Shvareva, and A. Navrotsky: Thermochemistry of lanthana- and yttria-doped thoria. *J. Am. Ceram. Soc.* **93**, 4142–4147 (2010).
33. P-L. Chen and I-W. Chen: Role of defect interaction in boundary mobility and cation diffusivity of CeO_2. *J. Am. Ceram. Soc.* **77**, 2289–2297 (1994).
34. P-L. Chen and I-W. Chen: Grain boundary mobility in Y_2O_3: defect mechanism and dopant effects. *J. Am. Ceram. Soc.* **79**, 1801–1809 (1996).
35. P-L. Chen and I-W. Chen: Grain growth in CeO_2: dopant effects, defect mechanism, and solute drag. *J. Am. Ceram. Soc.* **79**, 1793–1800 (1996).
36. Y. Dong, H. Wang, and I.W. Chen: Electrical and hydrogen reduction enhances kinetics in doped zirconia and ceria. I. Grain growth study. *J. Am. Ceram. Soc.* **100**, 876–886 (2017).
37. M. Biesuz and V.M. Sglavo: Flash sintering of alumina: effect of different operating conditions on densification. *J. Eur. Ceram. Soc.* **36**, 2535–2542 (2016).

https://doi.org/10.1557/mrc.2017.70 Published online by Cambridge University Press